13

Theoretical analysis of a gyrotron driven by an external harmonic signal

© N.V. Grigorieva,[1,2] A.G. Rozhnev,[1,2] N.M. Ryskin[1,2]

[1] Saratov Branch, Kotel'nikov Institute of Radio Engineering and Electronics, Russian Academy of Sciences, 410019 Saratov, Russia
[2] Saratov National Research State University, 410012 Saratov, Russia
e-mail: preobnv@gmail.com

Received January 16, 2024
Revised January 16, 2024
Accepted January 16, 2024

In this paper, synchronization of a gyrotron by an external harmonic signal is analyzed based on a model with the Gaussian fixed structure of a high-frequency field using preliminary calculated complex gain factor. Stability conditions of the synchronization regimes with variation of beam current and cyclotron resonance mismatch are analyzed at different values of the driving amplitude. The dependences of the transversal efficiency (i.e., the portion of transverse energy given by electrons to the field) on these parameters are plotted. Optimal parameter values have been found at which, in the synchronization regime, an efficiency close to the maximal for an autonomous gyrotron is achieved, and a wide synchronization band is also ensured.

Keywords: gyrotron, synchronization, injection locking, bifurcation.

DOI: 10.21883/0000000000

Introduction

Cyclotron resonance masers, in particular gyrotrons, provide the highest power output levels in the millimeter and submillimeter wavelength ranges [1]. Currently, the electron cyclotron plasma heating in controlled thermonuclear fusion plants is one of the most important applications of gyrotrons [1–5]. Complexes of a large number of gyrotrons are usually used for these purposes, therefore it is important task to ensure their coherent operation. In particular, the idea of synchronizing a powerful gyrotron with a gyrotron driver signal with a stabilized frequency attracted attention [6,7]. Quasi-optical mode converters that convert an external signal into the operating mode of the gyrotron resonator have been developed for solving this problem [7,8]. Demonstration experiments were conducted in the lower frequency range of 35 GHz [9], and an experiment has been conducted most recently for synchronization of a powerful gyrotron with a frequency of 170 GHz under the impact of the input signal of a stabilized gyrotron driver [10].

The gyrotron synchronization by an external signal was theoretically studied earlier in many papers (see, for example, [11–21]), mainly using numerical modeling based on various models of the nonstationary theory of the gyrotron. In particular, it was found that exposure to an external signal helps to suppress parasitic modes and in some cases contributes to an increase of the generation efficiency [17–20]. However, building a detailed picture of synchronization using computer modeling is a very time-consuming task, especially in the presence of several interacting modes since this system is characterized, generally speaking, by a large number of control parameters. In this regard, it is of obvious interest to study the fundamental laws of gyrotron synchronization using methods of oscillation theory and nonlinear dynamics.

The study of the nonlinear dynamics of a gyrotron with a fixed structure of a radio-frequency (RF) field can be significantly simplified using the approach developed in Ref. [22–25]. This approach is based on the fact that the electron susceptibility, which determines the power of the interaction of the beam with the field, is expressed as a function of the amplitude of the field using interpolation of pre-calculated dependencies. In this case, the description is reduced to a dynamic system with one degree of freedom, for which the main results can be obtained, essentially analytically, without numerical integration of differential equations describing the dynamics of an electron beam under the action of an RF field. Specifically, the analysis of mutual [22,23] and forced [24,25] synchronization of gyrotrons was carried out based on this technique. It should be noted that the synchronization pattern depending on the amplitude and frequency of the external signal was studied in Ref. [24,25]. However, it is customary in the theory of the gyrotron to analyze the generation modes on the plane of the parameters of the magnetic field-beam current (see, for example, [17–21]). The results of such an analysis in relation to the gyrotron synchronization problem are provided in this paper. The main attention is paid to the possibilities of increasing efficiency in case of external signal impact.

1. Model and basic equations

Let's use the well-known equations of the nonstationary theory of a gyrotron with a fixed RF field structure (see, for example, [21]). The field in the resonator in this case can

be represented as the product of a complex amplitude A, slowly changing in comparison with the eigen frequency, and the function $f(\xi)$, which describes the distribution of the field in the resonator (ξ — dimensionless longitudinal coordinate). For simplicity, let's limit ourselves to the interaction of an electron beam with a single resonator mode on the fundamental cyclotron harmonic. Then the equation of electron motion and boundary conditions will be written as follows:

$$\frac{dp}{d\xi} + i\left(\Delta_H + |p|^2 - 1\right)p = iAf(\xi),$$

$$p(\xi = 0) = e^{i\phi_0}. \quad (1)$$

Here p — normalized transverse momentum, Δ_H — cyclotron resonance mismatch proportional to the difference between the eigen frequency of the operating mode of the resonator ω_0 and the cyclotron frequency ω_H, ϕ_0 — the initial phases of electrons, which are considered to be uniformly distributed over the interval $[0; 2\pi]$.

The dynamics of the oscillation amplitude is described by the resonator excitation equation

$$\frac{dA}{d\tau} + A = iI_0 \int_0^{\xi_L} J(\xi, \tau) f^*(\xi) d\xi. \quad (2)$$

Here τ — dimensionless time, I_0 — a parameter that makes sense of the normalized electron beam current, ξ_L — the length of the interaction space,

$$J = \frac{1}{2\pi} \int_0^{2\pi} p d\phi_0 \quad (3)$$

— the complex amplitude of the RF harmonic current, the symbol «*» indicates a complex conjugate. All variables in (1)–(3) are dimensionless, the normalization of variables is described in detail in Ref. [22–25].

There is an approach that can significantly simplify the analysis of self-oscillations in a gyrotron with a fixed RF field structure. We introduce a complex function of electronic susceptibility

$$\Phi = \frac{i}{A} \int_0^{\xi_L} J(\xi, \tau) f^*(\xi) d\xi, \quad (4)$$

which determines the power of the interaction of the beam with the resonator field. If we perform a series of calculations using equations (1) for different values of cyclotron resonance mismatch Δ_H and field amplitude A, and then interpolate the calculated dependencies, then the susceptibility can be expressed as a function of two variables: $\Phi = \Phi(|A|, \Delta_H)$. Then the excitation equation (2) has the following form

$$\frac{dA}{d\tau} + A = I_0 \Phi(|A|, \Delta_H) A. \quad (5)$$

Therefore, for describing the dynamics of oscillations in a gyrotron, we obtain a dynamic system with one degree of freedom, the study of which is greatly simplified. Ref. [22–25] showed that the results obtained using this approach are completely consistent with the results of numerical modeling based on the equations of the nonstationary theory of a gyrotron with a fixed field structure (1)–(3).

Figure 1 shows the real (active) and imaginary (reactive) parts of the electron susceptibility calculated for the case of a Gaussian field distribution in a resonator

$$f(\xi) = \exp\left[-3\left(\frac{2\xi}{\xi_L} - 1\right)^2\right] \quad (6)$$

at $\mu = 15.0$, where $\mu = \xi_L/\sqrt{3}$ is a dimensionless parameter determining the width of the RF field distribution by level e^{-1}.

It should be noted that the following equations follow from (5) in the stationary generation mode, when it is possible to put $A = a_0 \exp(i(\Omega_0 \tau + \varphi_0))$, where a_0, Ω_0 and φ_0 are considered real

$$I_0 \mathrm{Re}\Phi(a_0, \Delta_H) = 1,$$

$$\Omega_0 = I_0 \mathrm{Im}\Phi(a_0, \Delta_H) = \frac{\mathrm{Im}\Phi(a_0, \Delta_H)}{\mathrm{Re}\Phi(a_0, \Delta_H)}, \quad (7)$$

determining the amplitude and frequency of the oscillation.

It is not difficult to generalize the theoretical model described above to the situation when the gyrotron is under the impact of an external signal. In this case, equation (5) is modified as follows (see, for example, [18,19,24,25]):

$$\frac{dA}{d\tau} + A = I_0 \Phi(|A|, \Delta_H) A + 2Fe^{i\Omega\tau}. \quad (8)$$

Here F is the amplitude of the external signal, and Ω is the dimensionless mismatch between the frequency of the external signal and the eigen frequency of the resonator ω_0. It is possible to show that we have $F/|A| \approx \sqrt{P_{in}/P_{out}}$ with the selected normalization of the amplitude of the external signal, where P_{in} — the power of the external signal, P_{out} — the output power of the gyrotron [12,19]. It is convenient to make a replacement $A = a(\tau)\exp\left(i(\Omega\tau + \varphi(\tau))\right)$. Then a system of two real equations follows from (8)

$$\frac{da}{d\tau} + a = I_0 \mathrm{Re}\Phi(a, \Delta_H) a + 2F\cos\varphi,$$

$$\frac{d\varphi}{d\tau} + \Omega = I_0 \mathrm{Im}\Phi(a, \Delta_H) - \frac{2F}{a}\sin\varphi. \quad (9)$$

A theoretical analysis of synchronization modes was conducted based on the model (9) in Ref. [24,25] and the main bifurcation mechanisms resulting in the setting of synchronous modes were identified. At the same time, this model allows calculating the values of quantitative parameters that are important from a practical point of view, such as efficiency, synchronization bandwidth, etc.

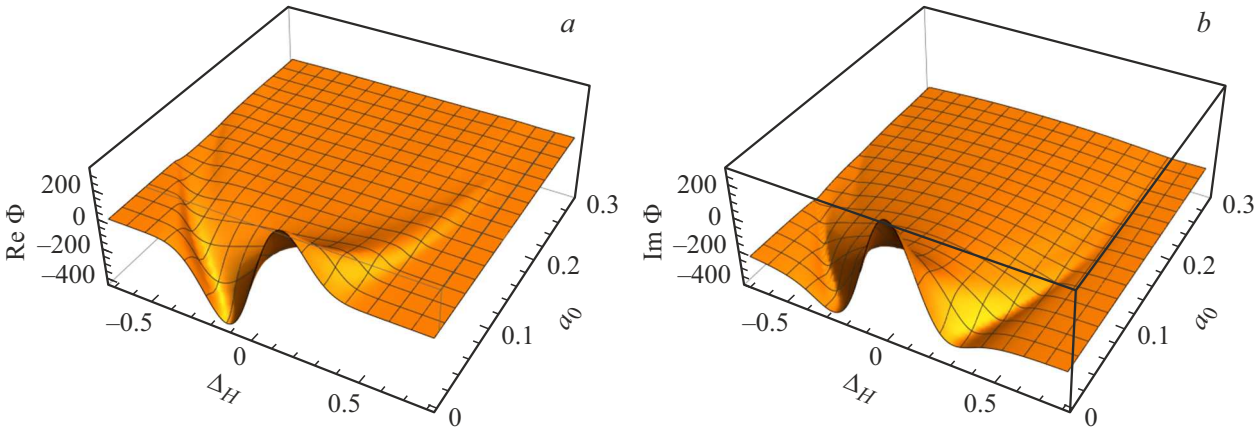

Figure 1. Dependences of active (a) and reactive (b) electronic susceptibility on the amplitude of oscillations a_0 and the cyclotron resonance mismatch Δ_H at $\mu = 15$.

2. Conditions for the stability of synchronization modes

Let's consider the synchronization mode, when fluctuations are set at the frequency of external driving with a constant amplitude. They correspond to the fixed points of the system (9) $a = a_0$, $\varphi = \varphi_0$. In this case, the following relations are derived from (9)

$$1 - I_0 \mathrm{Re}\Phi(a_0, \Delta_H) = \frac{2F}{a_0} \cos\varphi_0,$$

$$\Omega - I_0 \mathrm{Im}\Phi(a_0, \Delta_H) = -\frac{2F}{a_0} \sin\varphi_0, \qquad (10)$$

which, at $F = 0$, obviously pass into (7). It is possible to obtain the equation of resonant curves if φ_0 phase is excluded from (10)

$$\left(1 - I_0 \mathrm{Re}\Phi(a_0, \Delta_H)\right)^2 + \left(\Omega - I_0 \mathrm{Im}\Phi(a_0, \Delta_H)\right)^2 = \frac{4F^2}{a_0^2}. \qquad (11)$$

The stability conditions of fixed points can be found by using a standard procedure for linearization of equations (9) (for more details, see [24,25]). As a result, it is possible to obtain a characteristic equation of the following form

$$p^2 + 2kp + n = 0, \qquad (12)$$

where the following notation is introduced

$$k = 1 - I_0 \mathrm{Re}\Phi(a_0, \Delta_H) - I_0 \frac{\partial \mathrm{Re}\Phi(a_0, \Delta_H)}{\partial a_0} a_0^2, \qquad (13)$$

$$n = \left[1 - I_0 \mathrm{Re}\Phi(a_0, \Delta_H) - I_0 \frac{\partial \mathrm{Re}\Phi(a_0, \Delta_H)}{\partial a_0} a_0^2\right]^2 + \left[\Omega - I_0 \mathrm{Im}\Phi(a_0, \Delta_H) - I_0 \frac{\partial \mathrm{Im}\Phi(a_0, \Delta_H)}{\partial a_0} a_0^2\right]^2 - I_0^2 \left[\left(\frac{\partial \mathrm{Re}\Phi(a_0, \Delta_H)}{\partial a_0}\right)^2 + \left(\frac{\partial \mathrm{Im}\Phi(a_0, \Delta_H)}{\partial a_0}\right)^2\right] a_0^4. \qquad (14)$$

The fixed point is stable at $\mathrm{Re}p < 0$, which occurs when the conditions $k > 0$ and $n > 0$ are met.

Therefore, it is possible to construct the boundaries of the stability domain in the space of control parameters. The ratio $n = 0$ gives the boundary of the saddle node bifurcation, i.e. the boundary of the merging and disappearance of two fixed points. The ratio $k = 0$ defines the boundary of the Andronov-Hopf bifurcation, i.e. the bifurcation of the birth of the limit cycle from a fixed point. These bifurcations correspond to the known mechanisms of frequency locking and suppression of natural dynamics in the context of the problem of synchronizing the generator with an external harmonic signal [26,27].

The pattern of resonance curves was analyzed in Ref. [24,25], depending on the parameters of the external signal F and Ω. However, as already noted, the analysis is more interesting depending on the parameters I_0 and Δ_H, i.e., in fact, depending on the beam current and the magnetic field.

3. Simulation results

Let's first consider an autonomous gyrotron. Fig. 2, *a* shows the dependences of the field amplitude on the cyclotron resonance mismatch at different values of the parameter I_0. The values of the transverse electron efficiency (i.e., the proportion of rotational energy given by electrons to the field) are of greater interest from a practical point of view

$$\eta = 1 - \frac{1}{2\pi} \int_0^{2\pi} |p(\xi_L)|^2 d\varphi_0. \qquad (15)$$

It is not difficult to show (see, for example, [12,21–25]) that in stationary mode, efficiency is associated with active susceptibility by the ratio

$$\eta = 2\mathrm{Re}\Phi(a_0, \Delta_H) a_0^2. \qquad (16)$$

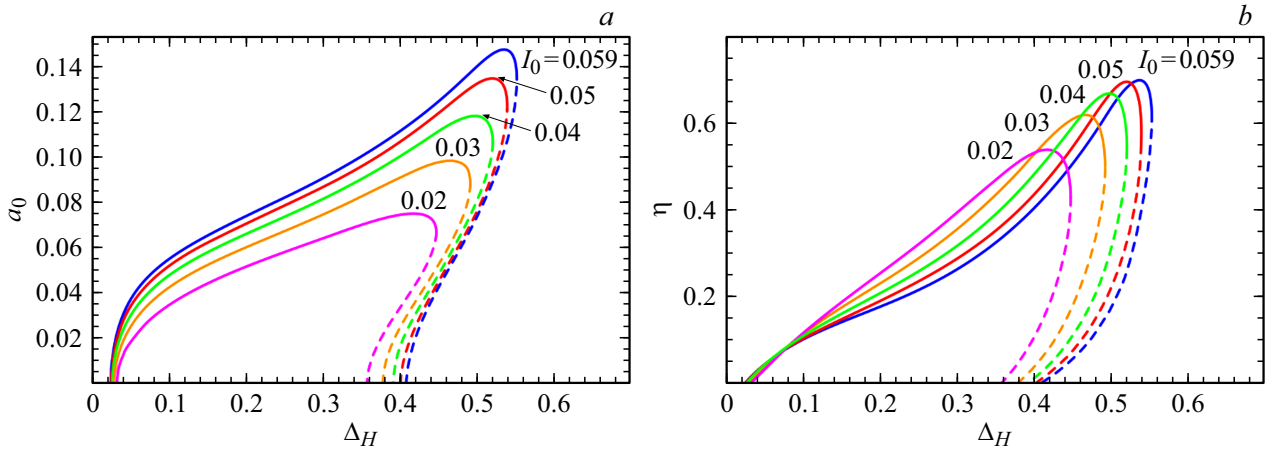

Figure 2. Dependences of amplitude (a) and transverse efficiency (b) on the cyclotron resonance mismatch of an autonomous gyrotron with different current values. Stable states are shown by solid lines, unstable states are shown by dashed lines.

The corresponding dependencies are shown in Fig. 2, b. It can be seen that the maximum efficiency shifts to the area of large mismatch with an increase of current. The absolute maximum efficiency of $\eta_{\max}$ can be found from the conditions $\partial\eta/\partial a_0 = 0$, $\partial\eta/\Delta_H = 0$. At chosen value of the dimensionless length of the interaction space ($\mu = 15.0$) $\eta_{\max} \approx 0.706$ is achieved with $\Delta_H = \Delta_{\max} \approx 0.534$ and $a_0 = a_{\max} \approx 0.144$ and these values do not change even in the presence of an external signal.

It can also be concluded based on Fig. 2 that dependencies become multivalued with increase of the detuning. The state with a larger amplitude value is stable in this case, the state with smaller amplitude is unstable [24,25], and, additionally, the zero solution is stable. This situation corresponds to the hard excitation of oscillations [24–28]. It should be noted that the maximum possible efficiency is achieved in the hard excitation mode.

Also, the „hot" eigen frequency can be determined from the second equation of the system (7). $\Omega_0(a_{\max}, \Delta_{\max}) \approx -0.75$ in the maximum efficiency point. The frequency of external driving should be close to this value for achieving the maximum efficiency value in the synchronization mode.

Let's choose the value of the frequency of the external signal $\Omega = -0.75$, which is close to the value of $\Omega_0(a_{\max}, \Delta_{\max})$, and the value of the normalized current $I_0 = 0.02$, i.e. about three times lower than that at which the maximum efficiency is achieved in an autonomous gyrotron. Let's consider the synchronization modes at different values of the amplitude of the external signal. Fig. 3, a shows the dependences of the oscillation amplitude on Δ_H. Qualitatively, they are similar to the pattern of the resonant curves of the Van der Pol–Duffing self-excited oscillator under external impact, which is described in detail in the literature (see, for example, [21,26,27]). It should be noted that the dependencies $a_0(\Delta_H)$ have a simpler and more understandable structure than the dependencies $a_0(\Omega)$ for the case of hard excitation, presented in [24–28]. At low F, the resonance curves consist of two branches. The lower branch corresponds to the mode of forced oscillations with a small amplitude and is located near the horizontal axis. The upper branch corresponds to the locking mode. It encircles the point at which the resonance curves (11) degenerate at $F = 0$. The lower branch connects with the upper branch with an increase of F. Obviously, this situation is most favorable from a practical point of view, since the synchronization mode is stable over a fairly wide range of changes in the cyclotron resonance mismatch. The stability boundaries are also plotted on Fig. 3, i.e. curves on which the conditions of saddle node bifurcation (SN) and Andronov-Hopf bifurcation (AH) are fulfilled, which are determined by the conditions $n = 0$ and $k = 0$, respectively. The first of them is a closed curve that intersects the dependencies $a_0(\Delta_H)$ at those points where the tangent to them is vertical.

The amplitude of the oscillations increases when moving along the resonant curve as Δ_H increases and reaches its maximum value, then the amplitude of the oscillations begins to decrease and reaches the point of saddle node bifurcation. An abrupt decrease of amplitude occurs in this point. The transition to the mode with a large amplitude occurs at a lower value of Δ_H in case of movement in the opposite direction of the parameter, i.e. hysteresis occurs. AH bifurcation will occur with a further decrease of the detuning. The instability in this region is associated with the soft occurrence of beats, i.e. quasi-periodic oscillations (see [28]).

Fig. 3, b shows the corresponding dependencies for efficiency. It can be seen that the maximum efficiency increases with an increase of the amplitude of the impact. So, we have $\eta = 0.69$ for $Delta_H \approx 0.53$ and $F = 0.05$, which is close to the maximum possible value of $\eta_{\max}$ and significantly more than in an autonomous gyrotron at $I_0 = 0.02$, where $\eta \leq 0.54$. It should be noted that the power of the external signal is approximately 10% of the generation power of the autonomous gyrotron.

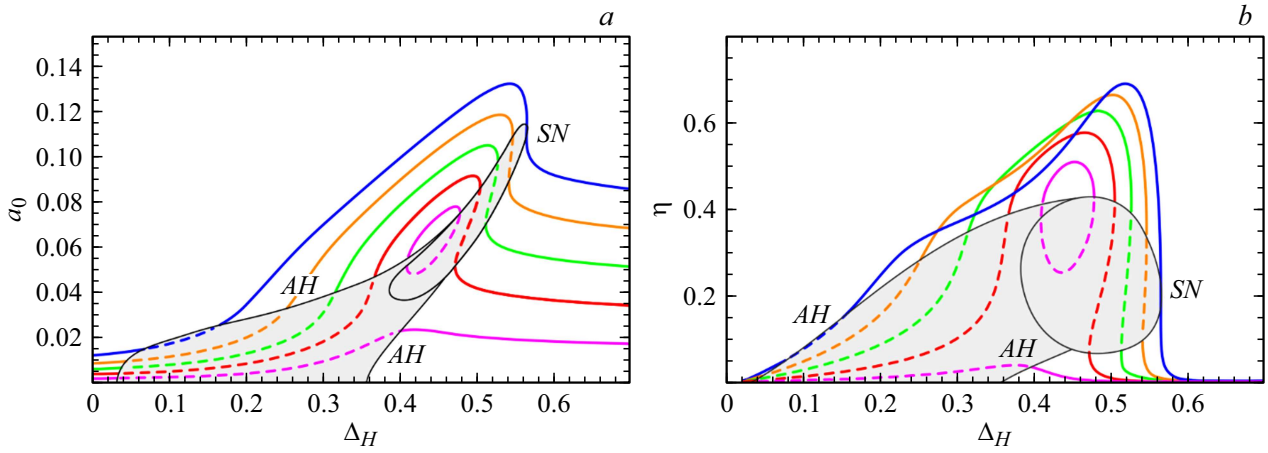

Figure 3. Dependences of amplitude (a) and transverse efficiency (b) on the cyclotron resonance mismatch for a non-autonomous gyrotron at $I_0 = 0.02$, $\Omega = -0.75$ and various values F: purple curve — 0.01, red curve — 0.02, green curve — 0.03, orange curve — 0.04, blue curve — 0.05. Stable states are shown by solid lines, unstable states are shown by dashed ones, instability areas are shaded in gray.

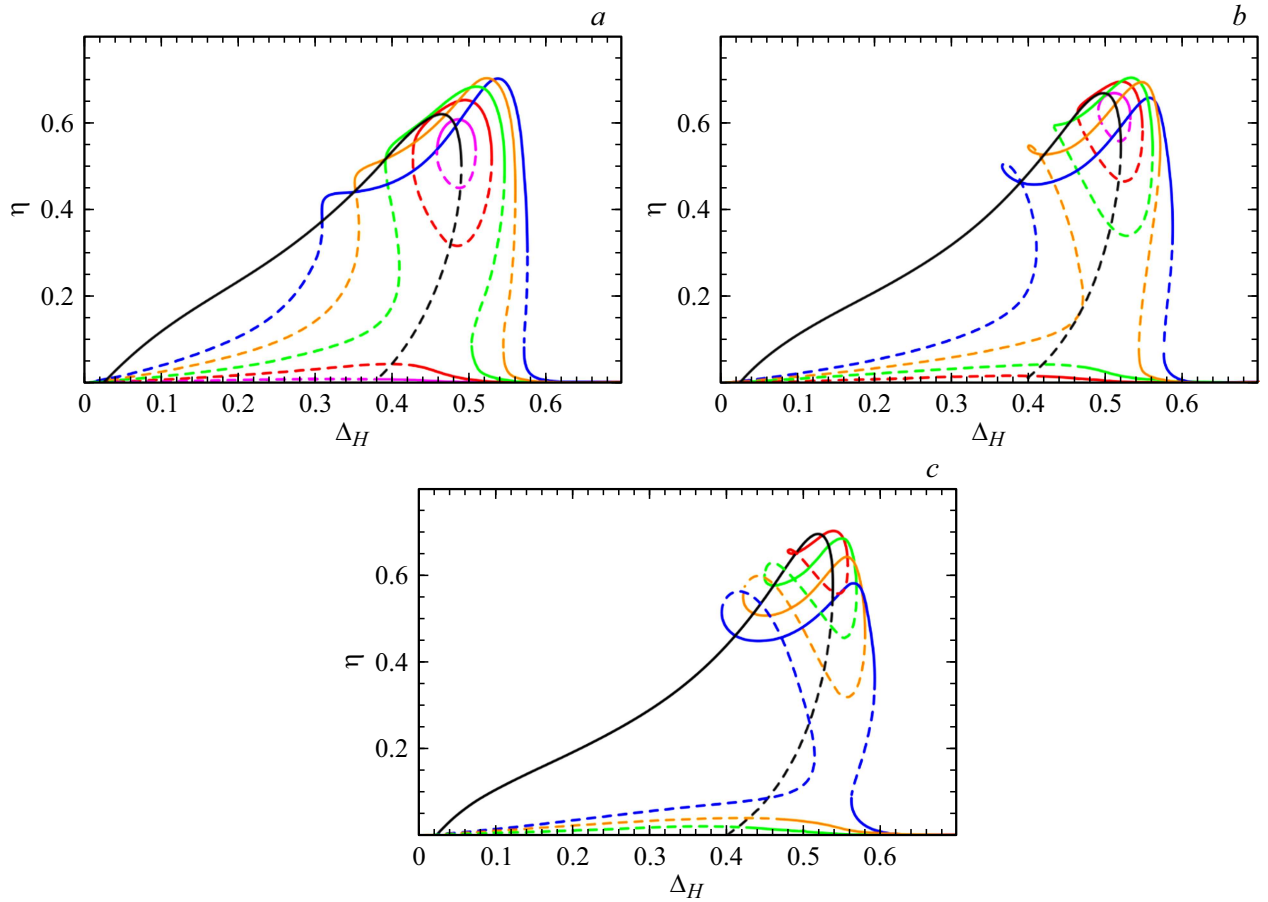

Figure 4. Dependences of transverse efficiency on cyclotron resonance mismatch at $\Omega = -0.75$ and $I_0 = 0.03$ (a), $I_0 = 0.04$ (b), $I_0 = 0.05$ (c) and various values of the amplitude of the external signal: purple curve — $F = 0.01$, red curve — 0.02, green curve — 0.03, orange curve — 0.04, blue curve — 0.05. The dependencies for the autonomous gyrotron are shown in black. Stable states are shown by solid lines, unstable states are shown by dashed lines.

Figure 4 shows the dependence of efficiency on mismatch, plotted with other values of the parameter I_0. The dependencies $\eta(\Delta_H)$ for an autonomous gyrotron are also provided for comparison. It can be seen that the power of

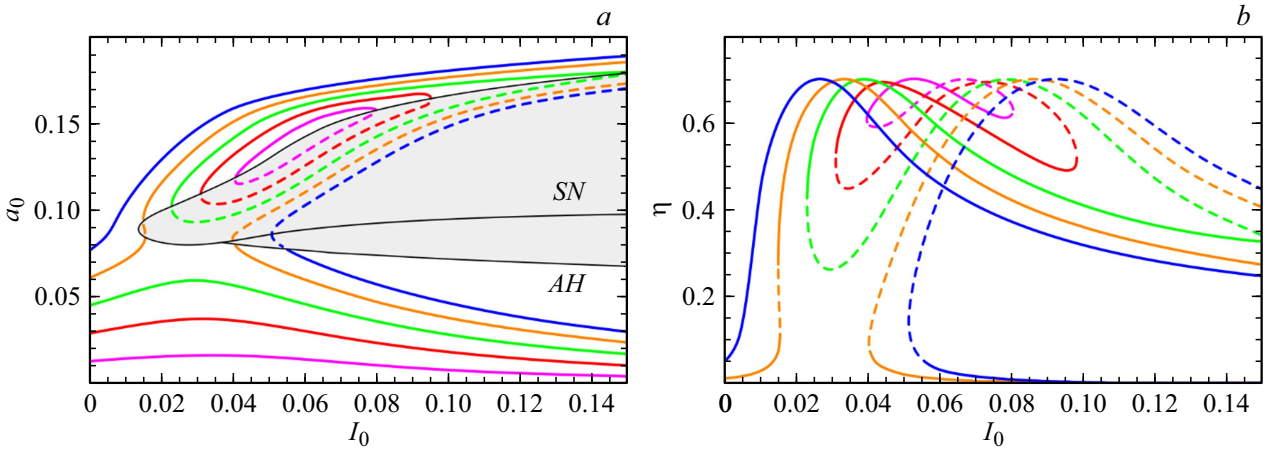

Figure 5. Dependences of amplitude (a) and transverse efficiency (b) on the normalized current at $\Delta_H = 0.534$, $\Omega = -0.75$ and different values of the amplitude of the external signal (the same values are selected F, as in Fig. 3, 4). Stable states are shown by solid lines, unstable states are shown by dashed lines.

the external signal at which maximum efficiency is achieved decreases with the increase of the current. However, the synchronization band becomes narrower in this case. Moreover, the shape of the resonance curves becomes more complicated, and dips are formed on them. The resonance curves has the form of lemniscate at currents close to the values at which optimal efficiency values are achieved in an autonomous gyrotron (Fig. 4, c). The reasons for this transformation were described in Ref. [25]. A similar behavior was also observed in the case of gyrotron synchronization by pre-modulation of the electron beam [11,21]. In general, it seems it is more efficient that from the point of view of synchronization to work at a current significantly lower than the current at which maximum efficiency is achieved in an autonomous gyrotron. At the same time, it is possible to significantly increase efficiency and provide a synchronization band comparable in width to the generation zone of an autonomous gyrotron.

It should also be noted that the area of detuning at which high efficiency values are achieved shifts to the right with an increase of F and is outside the generation zone of the autonomous gyrotron. In this case, we actually do not deal with synchronization, but with a regenerative amplification mode (for more information, see [25,28]).

It is also helpful to analyze the dependences of the oscillation amplitude and efficiency on the normalized beam current. Let's choose a fixed value of the cyclotron resonance mismatch $\Delta_H = \Delta_{\max} \approx 0.534$. A pattern of dependencies $a_0(I_0)$ is shown on Figure 5, a. The boundaries of the AH bifurcation and saddle node bifurcation are also plotted. Dependencies $a_0(I_0)$ consist of two branches. The upper branch is closed with a small amplitude of external driving. The structure of the resonance curves changes at $F \approx 0.036$: the branches overlap. It should be noted that multistability takes place in a certain range of the current parameter: one value I_0 corresponds to three values of the oscillation amplitude at once, two of which are stable. The state with a higher amplitude corresponds to the synchronization mode, the state with a lower amplitude corresponds to the forced oscillations mode with a small amplitude.

Fig. 5, b shows similar dependencies for efficiency. The dependencies $\eta(I_0)$ have the form of lemniscate in case of small values of F. There are also lower branches corresponding to forced oscillations with a small amplitude, but the efficiency for them does not exceed 0.01 and they are not shown in Fig. 5, b. The figure shows that the maximum value of efficiency $\eta_{\max}$ is reached with any amplitude of the external signal, and the lower is the F, the greater is the corresponding current value.

4. Conclusion

Gyrotron synchronization modes are theoretically investigated in this paper based on the model with a fixed field structure using approximations of pre-calculated functions of active and reactive electron susceptibility. The dependences of the oscillation amplitude and efficiency on the cyclotron resonance mismatch and the normalized electron beam current at different amplitudes of the external signal are analyzed. The results obtained show that the situation when the operating current of the gyrotron is significantly (by 2–3 times) lower than the current at which the maximum efficiency is achieved in an autonomous gyrotron. A similar situation is typical, in particular, for recent experiments with gyrotron synchronization with an auxiliary gyrotron driver with a stabilized frequency [10]. In this case, exposure to an external signal allows raising the efficiency to the maximum possible values and providing a wide synchronization band. At the same time, high efficiency values are achieved in the area of cyclotron resonance mismatch lying outside the autonomous gyrotron syhchronization zone, i.e., strictly speaking, not in synchronization mode, but in regenerative amplification mode.

In conclusion, it should be noted that the mode competition processes significantly influence the gyrotron dynamics. It is known that exposure to an external signal contributes to the suppression of parasitic modes [17–20]. Taking into account the interaction of modes significantly complicates the analysis of synchronization modes. However, the methodology used in the work can be adapted to analyze stability with respect to the excitation of parasitic modes. The results of such an analysis for an autonomous gyrotron with a quasi-equidistant mode spectrum were presented in Ref. [29]. Clarifying the synchronization pattern, taking into account the competition of modes, will be the subject of further research.

Funding

This study was supported by grant № 22-22-00603 from the Russian Science Foundation.

Conflict of interest

The authors declare that they have no conflict of interest.

References

[1] M. Thumm. J. Infrared Millim., Terahertz Waves, **41**, 1 (2020). DOI: 10.1007/s10762-019-00631-y
[2] M.K.A. Thumm, G.G. Denisov, K. Sakamoto, M.Q. Tran. Nucl. Fusion, **59**, 073001 (2019). DOI: 10.1088/1741-4326/ab2005
[3] A.G. Litvak, G.G. Denisov, M.Y. Glyavin. IEEE J. Microw., **1**, 260 (2021). DOI: 10.1109/JMW.2020.3030917
[4] R. Ikeda, K. Kajiwara, T. Nakai, T. Ohgo, S. Yajima, T. Shinya, Y. Mitsunaka, Y. Oda, T. Kobayashi, K. Takahashi, S. Moriyama, T. Eguchi, K. Sakamoto. Nucl. Fusion, **61**, 106031 (2021). DOI: 10.1088/1741-4326/ac21f7
[5] T. Rzesnicki, Z.C. Ioannidis, K.A. Avramidis, I. Chelis, G. Gantenbein, J.-P. Hogge, S. Illy, J. Jelonnek, J. Jin, A. Leggieri, F. Legrand, I.Gr. Pagonakis, F. Sanchez, M. Thumm. IEEE Electron Device Lett., **43**, 623 (2022). DOI: 10.1109/LED.2022.3152184
[6] G.G. Denisov, A.N. Kuftin, V.N. Manuilov, N.A. Zavolsky, A.V. Chirkov, E.A. Soluyanova, E.M. Tai, M.I. Bakulin, A.I. Tsvetkov, A.P. Fokin, Y.V. Novozhilova, B.Z. Movshevich, M.Yu. Glyavin. Microwave Opt. Technol. Lett., **62**, 2137 (2020). DOI: 10.1002/mop.32330
[7] G. Denisov, A. Kuftin, V. Manuilov, A. Chirkov, L. Popov, V. Zapevalov, A. Zuev, A. Sedov, I. Zheleznov, M. Glyavin. Nucl. Fusion, **62**, 036020 (2022). DOI: 10.1088/1741-4326/ac4946
[8] A.V. Chirkov, G.G. Denisov, A.N. Kuftin. Appl. Phys. Lett., **106**, 263501 (2015). DOI: 10.1063/1.4923269
[9] V.L. Bakunin, Yu.M. Guznov, G.G. Denisov, N.I. Zaitsev, S.A. Zapevalov, A.N. Kuftin, Yu.V. Novozhilova, A.P. Fokin, A.V. Chirkov, A.S. Shevchenko. Radiophys. Quant. Electron., **62**, 481 (2019). DOI: 10.1007/s11141-020-09994-y
[10] A.N. Kuftin, G.G. Denisov, A.V. Chirkov, M.Yu. Shmelev, V.I. Belousov, A.A. Ananichev, B.Z. Movshevich, I.V. Zotova, M.Yu. Glyavin. IEEE Electron Device Lett., **44**, 1563 (2023). DOI: 10.1109/LED.2023.3294755
[11] I.G. Zarnitsyna, G.S. Nusinovich. Radiophys. Quant. Electron., **18**, 339 (1975). DOI: 10.1007/BF01036701
[12] V.S. Ergakov, M.A. Moiseev, V.I. Khizhnyak. Radiotekhnika i elektronika, **23**, 2591 (1978) (in Russian).
[13] A.W. Fliflet, W.M. Manheimer. Phys. Rev. A, **39**, 3432 (1989). DOI: 10.1103/PhysRevA.39.3432
[14] A.H. McCurdy, A.K. Ganguly, C.M. Armstrong. Phys. Rev. A, **40**, 1402 (1989). DOI: 10.1103/ PhysRevA.40.1402
[15] P.E. Latham, B. Levush, G.S. Nusinovich, S. Parikh. IEEE Trans. Plasma Sci., **22**, 818 (1994). DOI: 10.1109/27.338297
[16] N.S. Ginzburg, A.S. Sergeev, I.V. Zotova. Phys. Plasmas, **22**, 033101 (2015). DOI: 10.1063/1.4913672
[17] V.L. Bakunin, G.G. Denisov, Yu.V. Novozhilova. Tech. Phys. Lett., **40**, 382 (2014). DOI: 10.1134/S1063785014050034
[18] V.L. Bakunin, G.G. Denisov, Yu.V. Novozhilova. Radiophys. Quant. Electron., **58**, 893 (2016). DOI: 10.1007/s11141-016-9663-0
[19] Yu.V. Novozhilova, G.G. Denisov, M.Yu. Glyavin, N.M. Ryskin, V.L. Bakunin, A.A. Bogdashov, M.M. Melnikova, A.P. Fokin. Izv. vuzov. Prikladnaya nelineynaya dinamika, **25** (1), 4 (2017) (in Russian). DOI: 10.18500/0869-6632-2018-26-6–68-81
[20] V.L. Bakunin, G.G. Denisov, Y.V. Novozhilova. IEEE Electron Device Lett., **41**, 777 (2020). DOI: 10.1109/LED.2020.2980218
[21] G.S. Nusinovich. *Introduction to the Physics of Gyrotrons* (The Johns Hopkins University Press, Baltimore, London, 2004)
[22] A.B. Adilova, N.M. Ryskin. Radiophys. Quant. Electron., **63**, 703 (2021). DOI: 10.1007/s11141-021-10091-x
[23] A.B. Adilova, N.M. Ryskin. Electronics, **11**, 811 (2022). DOI: 10.3390/electronics11050811
[24] N.V. Grigorieva. Izv. vuzov. Prikladnaya nelineynaya dinamika, **29**, 905 (2021) (in Russian). DOI: 10.18500/0869-6632-2021-29-6-905-914
[25] N.V. Grigorieva, N.M. Ryskin. Radiophys. Quant. Electron., **65**, 371 (2022). DOI: 10.52452/00213462_2022_65_05_406
[26] P.S. Landa. *Avtokolebaniya v sistemakh s konechnym chislom stepeney svobody* (Nauka, M., 2019) (in Russian).
[27] A.P. Kuznetsov, S.P. Kuznetsov, N.M. Ryskin. *Nelinejnye kolebaniya* (URSS, M., 2020)
[28] K.A. Yakunina, A.P. Kuznetsov, N.M. Ryskin. Phys. Plasmas, **22**, 113107 (2015). DOI: 10.1063/1.4935847
[29] A.B. Adilova, N.V.Grigoryeva, A.G. Rozhnev, N.M. Ryskin. Radiophys. Quant. Electron., **66**, 143 (2023). DOI: 10.1007/s11141-023-10282-8

Translated by A.Akhtyamov

Translated by A.Akhtyamov